Biobased Vanillic Acid and Ricinoleic Acid: Building Blocks for Fully Renewable Copolyesters

Claudio Gioia*, Maria Barbara Banella, Grazia Totaro, Micaela Vannini, Paola Marchese, Martino Colonna, Laura Sisti and Annamaria Celli

University of Bologna, Department of Civil, Chemical, Environmental and Materials Engineering, Via Terracini 28, Bologna, 40131, Italy

Received December 18, 2017; Accepted December 26, 2017

ABSTRACT: New fully biobased polyether/esters have been synthesized by a one-pot polymerization reaction of ricinoleic acid (RA), vanillic acid (VA) and ethylene carbonate (EC). In particular, EC selectively reacts with the phenolic group of VA to obtain *in-situ* 4-(2-hydroxyethoxy)-3-methoxybenzoate (EV), suitable for subsequent copolymerization with RA. The procedure was carried out in a single step, without any solvent. Chemical structure and thermal properties of the new materials were studied in order to explore relationships between composition and final performances. The combination of EV, bearing a rigid aromatic structure, with RA, characterized by high flexibility and potential biocidal activity, allows the production of a novel class of fully biobased aliphatic-aromatic polymers presenting tuneable thermal properties and suitable for a range of applications, for example, in active packaging and biomedical fields.

KEYWORDS: Biobased building blocks, vanillic acid, ricinoleic acid, copolyesters

1 INTRODUCTION

Driven by the sustainability issue, recent years have seen impressive progress in biobased production pathways from renewable raw materials to commercial goods and particularly to fully biobased plastics [1–4]. Among the most interesting chemical building blocks, aromatic compounds represent a broad class of molecules which are mostly derived from fossil feedstock. However, renewable routes to many aromatic products are now being consolidated [5–10], owing to the development of technologies for establishing successful biorefineries.

Vanillin and its derivatives are among the aromatic compounds that mostly evoke strong research interest in developing biobased production processes, which is also related to their great potential as polymer building blocks and as commodity chemicals [11, 12]. Moreover, since vanillin is one of the very few biobased aromatic building blocks available at an industrial scale from lignin, it possesses the potential to become a key intermediate for the synthesis of biobased polyesters endowed with elevated thermomechanical properties [13]. A review by Fache *et al.* [14] sums up all the scientific work carried out up to 2015 to prepare a wide range of vanillin-based polymers, among which are polyesters. Moreover, it is reported that vanillin can be used for the synthesis of epoxy polymers, as a substitute for bisphenol A [15], or for the synthesis of polycarbonates [16], or methacrylate resins with properties comparable to those of commercial vinyl ester-based thermosets [17, 18]. Vanillin can also be employed for the synthesis of novel polymeric materials with interesting properties such as thermotropic liquid crystalline materials [19], high-performance polybenzoxazine thermosets [20], antimicrobial polymer films [21, 22] and antioxidant biomaterials [23]. Meier and Firdaus [24] copolymerized vanillin derivatives with fatty acids and obtained thermoplastic materials with relatively high molecular weight (up to 17 kDa) and with a wide range of melting and glass transition temperatures ranging from 16 to 78 °C and from –37 to –14 °C, respectively.

Previously, we studied the homopolymerization of vanillic acid (PEV) performed by reaction with ethylene carbonate and subsequent solid state polymerization [25]. PEV is characterized by a high thermal transition, notable crystallinity, low molecular weight and brittleness; for these reasons it was copolymerized with ε-caprolactone to obtain fully biobased copolyester with tuneable thermal properties.

*Corresponding author: Claudio.Gioia2@unibo.it

DOI: 10.7569/JRM.2017.634191

© 2018 Scrivener Publishing LLC

The present study aims at widening the possibilities of exploiting vanillic acid as a biobased aromatic building block to build new copolymers with modulated properties according to their composition. Novel copolyesters have been prepared starting from ricinoleic acid, which is a hydroxylated unsaturated fatty acid derived from castor oil produced by the *Ricinus communis* plant [26]. Ricinoleic acid possesses four functionalities: a carboxylic moiety, a hydroxyl group, a C=C unsaturation and a long aliphatic chain. Such a unique structure has allowed castor oil to become a very attractive natural feedstock in biorefinery as an alternative to many fossil-based products. Nowadays, castor oil represents a main constituent in applications such as specialty soaps, adhesives, surfactants, cosmetics and personal care products, wax substitutes, inks, perfumes, plasticizers, paints and coatings, lubricant materials, including a wide range of polymeric materials, as well as in the food, fine chemical, and pharmaceutical industries [27, 28].

The carboxyl and the hydroxyl functional groups can be exploited for the preparation of polyesters while the unsaturation can be employed for the preparation of thermosets by means of crosslinking reactions, or to covalently link bioactive molecules [27]. Moreover, the dangling chain, acting as plasticizer, can influence the mechanical and physical properties of the final materials by reducing the glass transition temperature [29] or by imparting antimicrobial activity [27]. The self-polycondensation of ricinoleic acid (PRA), described in our previous study [30], leads to a viscous amorphous liquid at ambient temperature, with a very low glass transition temperature (–67 °C) and a superior antibacterial efficacy [27]. These features were exploited in the preparation of copolyesters [27] and electrospun fibers with poly(butylene succinate) (PBS) [30].

Considering therefore that both PEV and PRA homopolymers are materials with limited mechanical properties and restricted applicability, the strategy here was to combine the rigid aromatic structure of vanillic acid with the high flexibility and notable biocidal potential of ricinoleic acid to prepare new copolymers suitable for different kinds of applications, such as packaging.

2 EXPERIMENTAL

2.1 Materials

Vanillic acid (VA), ethylene carbonate (EC), potassium carbonate ricinoleic acid (RA), dibuthyltin oxide (DBTO), methanol (MeOH), sulfuric acid, sodium bicarbonate, ethyl acetate, magnesium sulfate (all from Aldrich, with purities of 99% or more, as declared by the manufacturer) were not purified before use. Methyl vanillate (MV) monomer and poly(ethylene vanillate) (PEV) homopolymer were previously synthesized in our laboratory [25].

2.2 Synthesis of Methyl Ricinoleate (MR)

Ricinoleic acid (14.9 g, 50 mmol), methanol (100 ml) and sulphuric acid (0.5 ml) were introduced in a 250-ml round-bottom flask equipped with a magnetic stirrer and a reflux column. The mixture was allowed to react at reflux overnight, then the methanol was removed under reduced pressure. The resulting oil was solubilized in 50 ml of ethyl acetate, washed with 50 ml of $NaHCO_3$ solution and subsequently with water (3 portions of 50 ml). Finally, the organic phase was collected, dried over $MgSO_4$ and the solvent removed under reduced pressure to obtain methyl ricinoleate (yield 98%).

2.3 Synthesis of Poly(ethylene vanillate-*co*-ricinoleic acid) Copolymers (P(EV-*co*-RA))

First, MV (1.82 g, 10 mmol), EC (0.968 g, 11 mmol), potassium carbonate (10 mg, 0.073 mmol), DBTO (5 mg, 0.02 mmol) and MR (different amounts of MR were used according to Table 1) were introduced into a 100-ml three-neck round-bottom flask equipped with a magnetic stirrer. Then the mixture was heated under nitrogen atmosphere at 190 °C for 3 hours. The pressure was then slowly reduced to 0.15 mBar while the temperature was gradually increased to 230 °C during 3 hours. Finally, the mixture was kept for a further 3 hours before collecting the polymer.

The copolymers are named with the P(EV-*co*-RA)-X/Y abbreviation, where EV indicates the units derived from benzoic acid, 4-(2-hydroxyethoxy)-3-methoxy methyl ester and RA indicates the units derived

Table 1 Molar fractions of EV and RA units and molecular weight of P(EV-*co*-RA) copolyesters and corresponding homopolymers.

Sample	F_{EV} [a]	F_{RA} [a]	$M_n \cdot 10^{-3}$ [b]	$M_w \cdot 10^{-3}$ [b]
PEV	1	–	4.7[a]	–
P(EV-*co*-RA)-70/30	0.70	0.30	4.0	12.5
P(EV-*co*-RA)-50/50	0.48	0.52	2.0	6.8
P(EV-*co*-RA)-20/80	0.14	0.86	3.0	8.0
PRA	–	1	2.7	8.0

[a]Determined by ^{1}H-NMR (Equations 1 and 2)
[b]Determined by GPC

© 2018 Scrivener Publishing LLC

from ricinoleic acid. X/Y is the molar feed ratio of vanillic acid-to-ricinoleic acid.

2.4 Characterization

The ^{1}H-NMR spectra were recorded at room temperature on samples dissolved in $CDCl_3/CF_3COOD$ (80/20 V/V) using a Varian Inova 600 spectrometer, the proton frequency being 600 MHz. The ^{13}C-NMR spectra were recorded at 150.8 MHz, with a Varian Inova 600 spectrometer, equipped with a direct broadband probe optimized for X detection, and obtained after accumulating at least 5000 scans with a digital resolution of 0.552 Hz/point, corresponding to a spectral width of 36199 Hz. The experiment used a pulse width of 3.95 μs, an acquisition time of 1.000 s and a relaxation delay of 3.000 s. The measurements were performed at 25 °C.

Molecular weights (expressed in equivalent polystyrene) were determined by gel permeation chromatography (GPC), using a Hewlett Packard Series 1100 liquid chromatography instrument equipped with a TSKgel SuperMultiporeHZ-M column. A mixture of $CHCl_3$/1,1,1,3,3,3-hexafluoro-2-propanol (HFIP) (95/5 V/V) was used as eluent and a calibration plot was constructed with polystyrene standards.

The thermogravimetric analysis (TGA) was performed using a PerkinElmer TGA 4000 thermobalance under nitrogen atmosphere (gas flow 40 ml min^{-1}) at 10 °C min^{-1} heating rate from 30 °C to 800 °C. The temperature of the maximum degradation rate (T_D), corresponding to the maximum of the differential thermogravimetric curve, was calculated.

The calorimetric analysis was carried out by means of a PerkinElmer DSC6, calibrated with high purity standards. The measurements were performed under a nitrogen flow. In order to cancel the previous thermal history, the samples (ca. 10 mg) were initially heated at 20 °C min^{-1} to different temperatures, varying from 150 to 300 °C according to the sample characteristics, kept at high temperature for 3 min and then cooled to –75 °C at 20 °C min^{-1}. After this thermal treatment, the samples were analyzed by heating them from –75 °C to 150–290 °C at 20 °C min^{-1} (2nd scan). During the cooling scan the crystallization temperature (T_c) and the enthalpy of crystallization (ΔH_c) were measured. During the 2nd scan, the melting temperature (T_m) and the enthalpy of fusion (ΔH_m) were determined. The glass transition temperature (T_g) was measured during a heating scan at 20 °C min^{-1} after quenching the molten sample in liquid nitrogen.

Data from wide angle X-ray diffraction (WAXD) were collected in the 2θ range 5–60° using an X'PertPro diffractometer, equipped with a copper anode (Ka radiation, l = 1.5418 Å) and an X'Celerator detector. WAXD analyses were performed on samples after the following thermal treatment in DSC: heating at 20 °C min^{-1} to different temperatures, varying from 150 to 300 °C according to the sample characteristics, 3 min of isotherm at this temperature and then cooling to room temperature at 20 °C min^{-1}.

Optical microscopy observations were performed using a Carl Zeiss Axioskop 2 optical polarizing microscope (POM) equipped with a Linkam THMS 600 hot stage. A video camera allowed image acquisition during the crystallization process. A small amount of sample was placed between a coverslip and a slide, heated up to different temperatures, ranging from 270 to 300 °C according to the sample characteristics, and held at high temperature for 1 min. Then the samples were cooled at 10 °C min^{-1} by means of a nitrogen flow to observe the crystallization process.

3 RESULTS AND DISCUSSION

3.1 Synthesis of the Copolymers

Ricinoleic acid, methyl vanillate and ethylene carbonate were polymerized in bulk by a one-pot reaction (Figure 1). According to a procedure previously reported [25], methyl vanillate and ethylene carbonate react to obtain *in-situ* ethylene vanillate, which subsequently can undergo homopolymerization to obtain poly(ethylene vanillate), or react with a polymerization partner (e.g., a carboxylic acid or ester). In particular, methyl vanillate was preferable, in comparison with vanillic acid, since carboxylic acids are able to react with carbonates, thus interfering with the reaction of the phenol and, therefore, with the stoichiometry of the reaction. Methyl ricinoleate was used as comonomer due to its natural origin and to its linear aliphatic structure, which is able to confer a notable level of flexibility to the macromolecular chain.

A combination of stiff segments, based on PEV structures, and aliphatic chains, based on ricinoleic acid, should allow obtainment of fully biobased copolyesters presenting tuneable thermomechanical properties. For this purpose, three copolymers presenting different ratios of EV and ricinoleic acid (EV/RA 70:30, 50:50 and 20:80 molar ratio) were synthesized in the presence of potassium carbonate and a transesterification catalyst (DBTO).

3.2 Molecular Analysis

As already described [25], PEV is insoluble in the GPC solvent and therefore it was only analyzed by ^{1}H-NMR. Table 1 reports the molecular weights of PEV, PRA and their copolyesters.

© 2018 Scrivener Publishing LLC

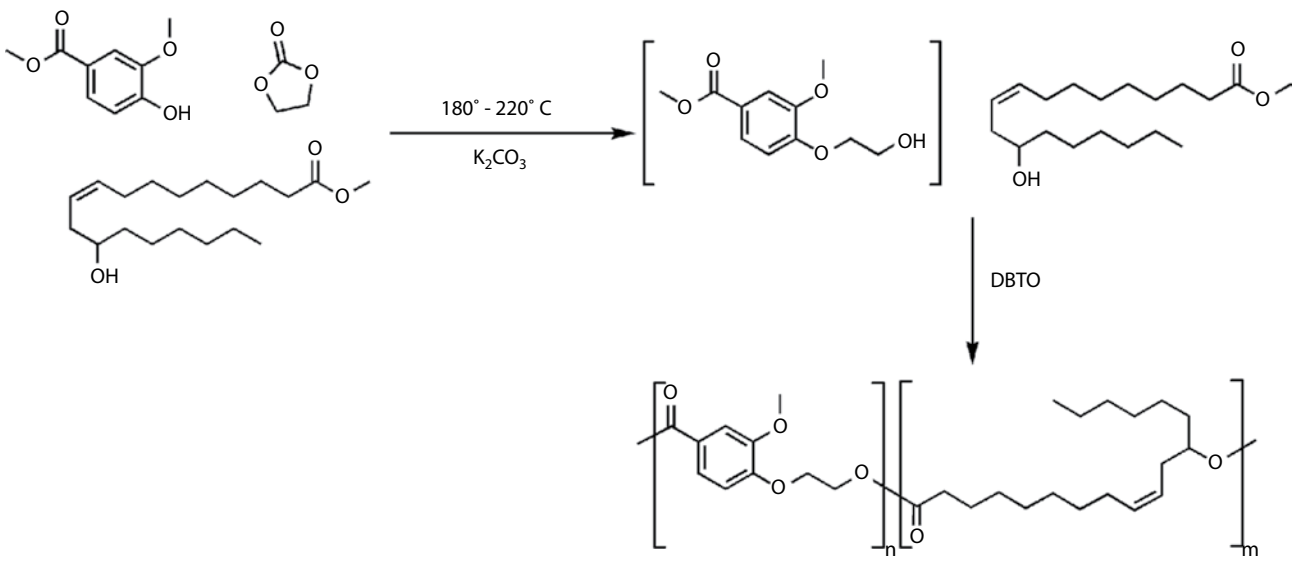

Figure 1 Synthetic pathway for the production of P(EV-*co*-RA) copolymers.

It is notable that the M_n and M_w values are rather low, suggesting that both 4-(2-hydroxyethoxy)-3-methoxybenzoate (EV) and methyl ricinoleate are characterized by a poor reactivity. In particular, a higher content of RA is associated with lower values of molecular weight. Such an effect is related to the lower reactivity of its secondary alcohol and the presence of a lateral aliphatic chain with a notable steric hindrance. However, in this work a classical two-stage polycondensation was used for the preparation of PRA, and a higher molecular weight was obtained in shorter times compared to those reported in the literature [31, 32].

This result differs from that obtain for P(EV-*co*-CL) copolymers [25], where the molecular weights increased with the amount of CL units, indicating a higher reactivity of the ε-caprolactone under those reaction conditions.

The new copolyesters were analyzed by ^{1}H-NMR to determine their molecular structure. In particular, Figure 2 represents a typical ^{1}H-NMR spectrum of P(EV-*co*-RA)-50/50. Peak assignments are based on the spectra recorded for PEV and PRA homopolymers, and on the literature for copolymers. It is notable that by comparing the integral values of the peak due to H_k and the sum of the peaks related to H_f and $H_{f'}$ the amount of double bond is maintained for every composition, despite the severe polymer conditions. Moreover, the ^{1}H-NMR spectra of the new copolymers are consistent with their expected structure.

Four different diads have been identified in the copolyester chains, namely (i) EV-EV sequence, obtained from the reaction between carboxylic and hydroxyl groups of the EV group; (ii) EV-RA sequence, obtained from the reaction between hydroxyl groups of the EV units and carboxylic groups derived from RA; (iii) RA-RA sequence, obtained from the reaction between the carboxylic and hydroxyl groups derived from RA; and (iv) RA-EV sequence, obtained from the reaction between hydroxyl groups derived from RA and carboxylic groups derived from EV units.

To determine the EV/RA composition, and therefore the molar fractions of EV (F_{EV}) and RA (F_{RA}), H_m (7.72–7.78 ppm) and H_k (0.88 ppm) were chosen since they are not affected by the chemical composition and are free from overlapping with other signals. F_{EV} and F_{RA} units were calculated by means of Equations 1 and 2, where I represents the integral of the signals:

$$F_{EV} = I_m / [\, I_m / (I_k / 3)] \quad (1)$$

$$F_{RA} = (I_K / 3) / (I_k + I_m) = 1 - F_{EV} \quad (2)$$

F_{EV} and F_{RA} values of the synthetized copolymers are reported in Table 1 and well reflect the feed composition.

In order to identify the average sequence lengths of EV-EV and RA-RA units and the randomness degree (B), some considerations regarding the NMR signals are necessary. The individual signals should be analyzed to identify which of them are affected by the copolymerization. Regarding PRA, H_f (5.31 ppm) and H_h are strongly subjected to splitting, and H_f is not completely resolved. Also, H_g and H_a are influenced by the copolymerization, but the overlapping is too strong. Finally, H_i (1.61 ppm) also splits, but $H_{i'}$ overlaps with it. Given these options, H_i appears to be the best proton to consider for the PRA units.

© 2018 Scrivener Publishing LLC

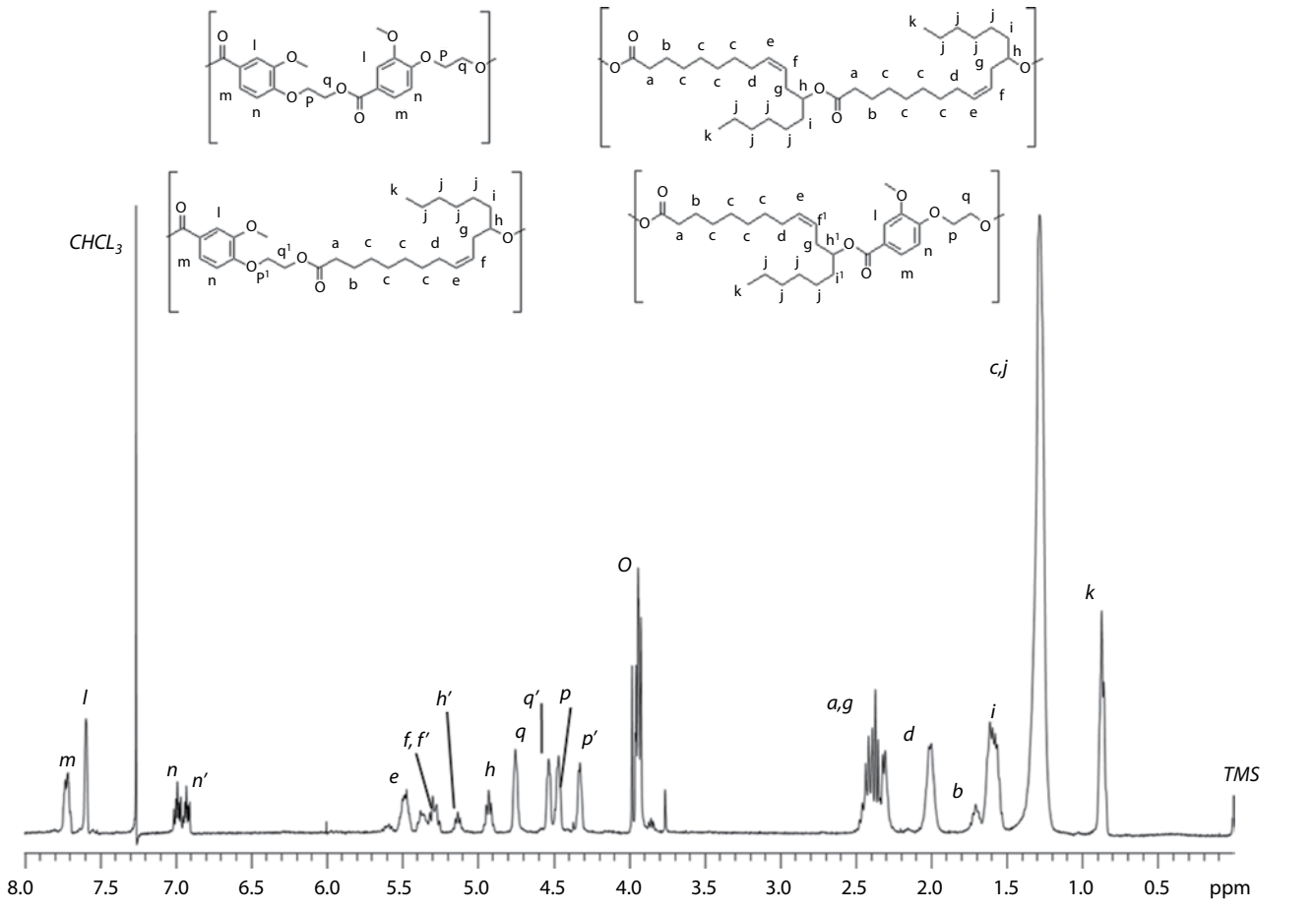

Figure 2 ^{1}H-NMR analysis of P(EV-co-RA)-50/50.

Regarding PEV, H_p (4.49 ppm), H_q (4.34 ppm) and H_n (7.01 ppm) splits can be well identified, but $H_{q'}$ and H_p chemical shifts are very close. Therefore, H_n intensity was selected.

The method reported by Devaux *et al.* [33] allows calculation of the molar fractions of diads (Equations 3, 4, 5, 6), average sequence lengths of EV-EV and RA-RA units (Equations 7, 8) and randomness degree (Equation 9).

$$F_{RA-RA} = \frac{I_h}{I_h + I_{h'}} \quad (3)$$

$$F_{EV-EV} = \frac{I_n}{I_n + I_{n'}} \quad (4)$$

$$F_{RA-EV} = \frac{I_{h'}}{I_{h'} + I_h} \quad (5)$$

$$F_{EV-RA} = \frac{I_{n'}}{I_{n'} + I_n} \quad (6)$$

Table 2 Average block lengths (L) and randomness degree (B) of P(EV-*co*-RA) copolyesters determined by ^{1}H- and ^{13}C-NMR.

	By ^{1}H-NMR			By ^{13}C-NMR		
Sample	L_{EV-EV}	L_{RA-RA}	B	L_{EV-EV}	L_{RA-RA}	B
P(EV-*co*-RA)-70/30	3.77	2.02	0.76	5.88	1.54	0.82
P(EV-*co*-RA)-50/50	2.16	2.77	0.82	2.74	2.23	0.81
P(EV-*co*-RA)-15/85	1.37	8.33	0.85	1.37	7.94	0.86

$$L_{EV-EV} = \frac{F_{EV-EV}}{F_{EV-RA}} + 1 \quad (7)$$

$$L_{RA-RA} = \frac{F_{RA-RA}}{F_{RA-EV}} + 1 \quad (8)$$

$$B = \frac{1}{L_{EV-EV}} + \frac{1}{L_{RA-RA}} \quad (9)$$

© 2018 Scrivener Publishing LLC

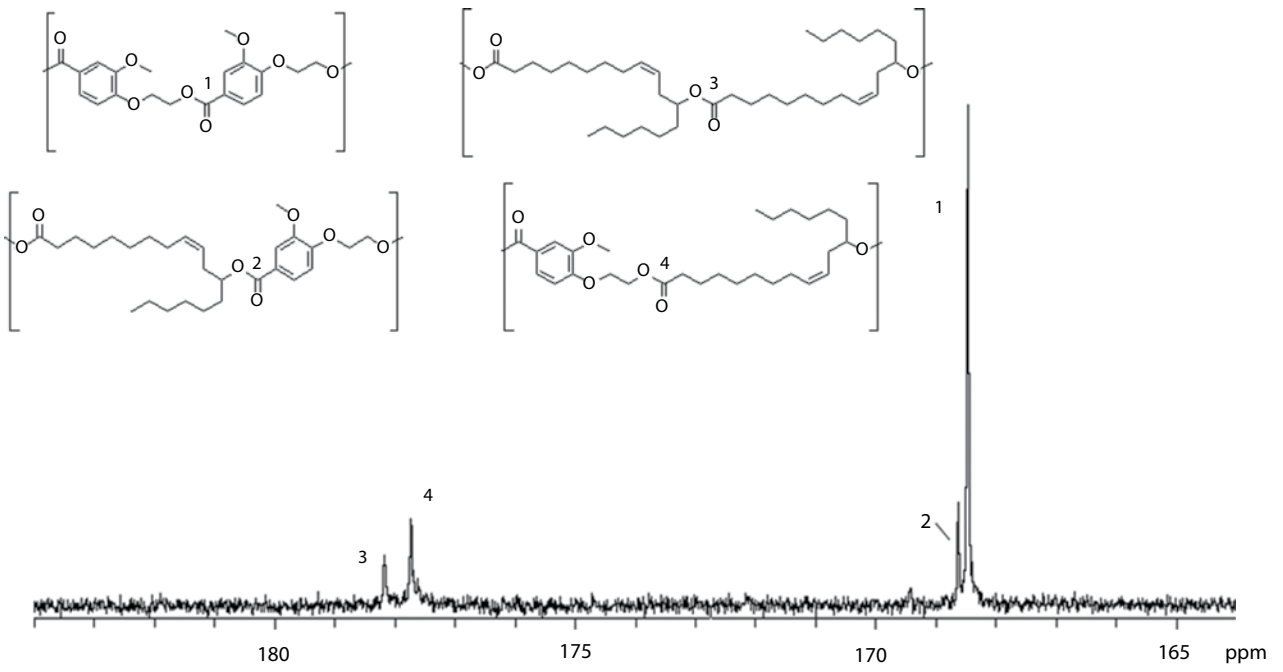

Figure 3 Expanded carbonyl region (165–185 ppm) of the ^{13}C-NMR spectrum of P(EV-co-RA)-70/30.

The values of L and B calculated by ^{1}H-NMR were compared with those obtained by ^{13}C-NMR (Table 2). More specifically, C_1 (168.5 ppm, EV-EV diad), C_2 (168.6 ppm, EV-RA diad), C_3 (177.7 ppm, RA-RA diad) and C_4 (178.2 ppm, RA-EV diad), belonging to four different carbonyl groups, were used to calculate the chemical sequences, according to Equations 10, 11, 12, 13, 14, 15, and 16 (Figure 3) [34–36].

As observed in Table 2, both methods to calculate L and B values from ^{1}H-NMR and ^{13}C-NMR provided similar results.

$$F_{EV-EV} = \frac{I_1}{I_1 + I_2} \quad (10)$$

$$F_{EV-RA} = \frac{I_2}{I_1 + I_2} \quad (11)$$

$$F_{RA-RA} = \frac{I_3}{I_3 + I_4} \quad (12)$$

$$F_{RA-EV} = \frac{I_4}{I_3 + I_4} \quad (13)$$

$$L_{EV-EV} = \frac{F_{EV-EV}}{F_{EV-RA}} + 1 \quad (14)$$

$$L_{RA-RA} = \frac{F_{RA-RA}}{F_{RA-EV}} + 1 \quad (15)$$

$$B = \frac{1}{L_{EV-EV}} + \frac{1}{L_{RA-RA}} \quad (16)$$

Moreover, the B values show that the sequence distribution of copolymers is best approximated as random and the sequence lengths vary following the random copolymer model according to the changes in composition.

3.3 Thermal and Morphological Analysis

The thermal stability of the samples was analyzed by TGA under nitrogen and the temperatures of the maxima of the differential thermogravimetric curves (T_D) are reported in Table 3. It is noteworthy that all the samples showed a high stability against degradation processes starting above 300 °C. Poly(ethylene vanillate) degraded in a single step at a higher temperature (T_D = 406 °C), whereas poly(ricinoleic acid) showed two separated peaks of decomposition at 360 and 450 °C, as previously reported [25, 27].

The degradation temperatures of the copolymers were located between those of the two homopolymers and the degradation process depended on the composition, as displayed in the thermogravimetric derivative curves reported in Figure 4.

© 2018 Scrivener Publishing LLC

Table 3 TGA and DSC characterization of P(EV-*co*-RA) copolyesters and corresponding homopolymers.

Sample[a]	T_D [a] (°C)	T_g [b] (°C)	T_c [c] (°C)	ΔH_c [c] (J·g^{-1})	T_m [d] (°C)	ΔH_m [d] (J·g^{-1})
PEV	406	73	156	61	264	68
P(EV-*co*-RA)-70/30	366-410	–18	142	35	255	35
P(EV-*co*-RA)-50/50	362-408-453	–44	99	18	n.d.[f]	n.d.[f]
P(EV-*co*-RA)-20/80	361-448	–60	–	–	–	–
PRA	360-450	–67[e]	–	–	–	–

[a] Determined by TGA under nitrogen at 10 °C min^{-1}
[b] Measured by DSC during the heating scan after quenching
[c] Measured by DSC during the cooling scan at 20 °C/min
[d] Measured by DSC during the 2nd heating scan at 20 °C/min
[e] ref. [19]
[f] not determinable due to the broad signal

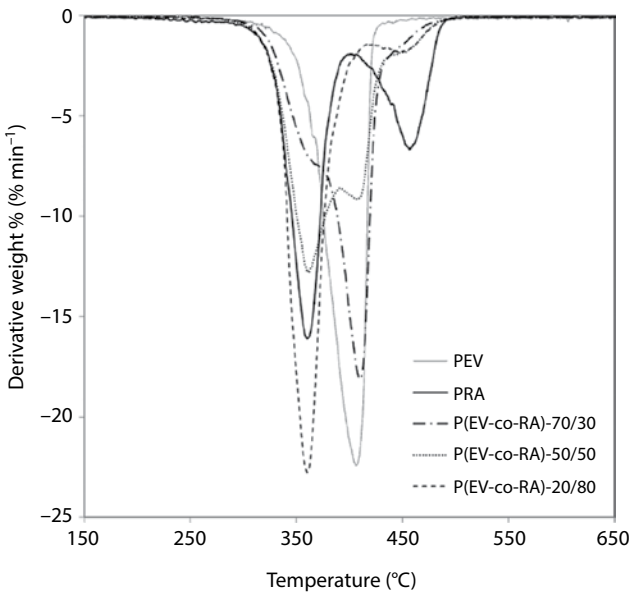

Figure 4 TGA curves of PEV, PRA and P(EV-*co*-RA) copolymers.

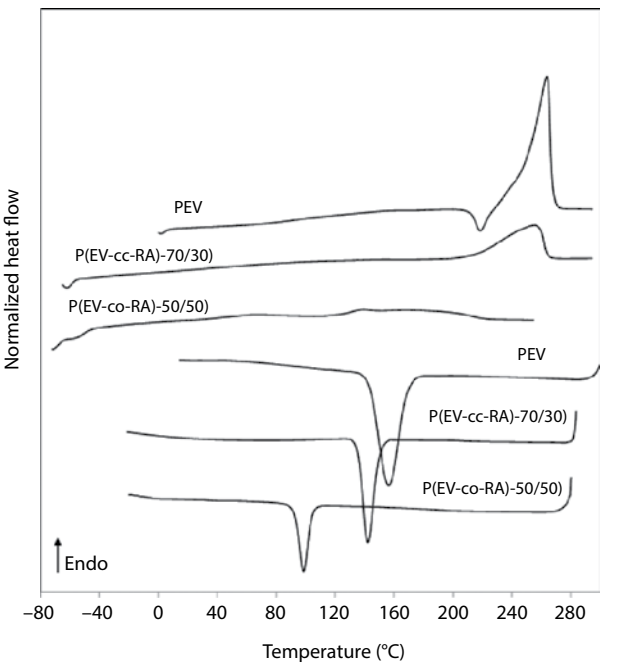

Figure 5 DSC scans of PEV and some P(EV-*co*-RA) copolymers.

P(EV-co-RA)-70/30 showed the first degradation process at a temperature close to that of PEV, but the presence of phenomena related to PRA sequences is also evident as a shoulder of the main process. For the P(EV-co-RA)-50/50 sample, both homopolymer degradation processes were noticeable and three peaks detected by TGA. A further increase in the amount of RA units led to a prevalence of PRA behavior and the curve of P(EV-co-RA)-20/80 sample was characterized by the two peaks observed for PRA. For this latter copolymer, the content of the EV units was too low (corresponding to 10 wt%) to allow evidence of PEV degradation. It is noteworthy that the T_D measured for the copolymers is similar to those of the homopolymers. The degradation phenomena of EV and RA co-units seems to be independent of the presence of the other comonomer.

The thermal properties were determined by DSC analysis according to the conditions described in the experimental section. Table 3 reports the results obtained during cooling and heating scans for PEV, P(EV-*co*-RA), and PRA samples [27]. These data show that PEV, P(EV-co-RA)-70/30 and P(EV-co-RA)-50/50 samples are semicrystalline while the P(EV-co-RA)-20/80 sample has a thermal behavior similar to that of the amorphous PRA. Crystallization and melting processes depend on the copolymers composition, as shown from the DSC cooling and subsequent heating scans reported in Figure 5.

© 2018 Scrivener Publishing LLC

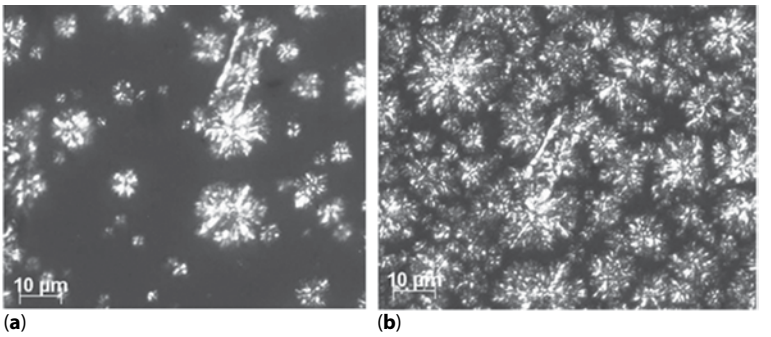

Figure 6 Optical microscopy observations on P(EV-*co*-RA)-50/50 sample at T=100 °C (**a**) and T=75 °C (**b**) during cooling from the melt.

The PEV crystallizes at high temperature (156 °C) with a high value of enthalpy (61 J g^{-1}), indicating a remarkable level of internal order reached after cooling from the melt, as discussed in a previous work [25]. Such a behavior has been justified by considering a higher mobility of the PEV chains around the rigid aromatic rings with respect to the terephthalic units in PET. Indeed, in PEV, where one carboxylic group is substituted by an ether unit, the coplanarity between two carbonyls and the phenyl groups is not present and this confers more mobility to the chain and can impart a higher chain-folding capability.

For P(EV-*co*-RA)-70/30 and 50/50 copolymers, the presence of ricinoleic acid units disturbs the crystallization of EV-segments resulting in a noticeable lowering of T_c (from 156 °C for PEV to 99 °C for the 50/50 sample). However, the crystallization process is fast, as shown by the narrow shape of crystallization peak observed during the cooling scan. The presence of RA units seems to have a remarkable influence on slowing down the first crystallization stage (nucleation), but this effect is not observed during the crystal growth process. The ΔH_c value of 70/30 sample is still sufficiently high considering the composition, indicating that the presence of 30 mol% of RA units has only a small effect on the final extent of crystallinity. An important decrement in ΔH_c is evident for P(EV-*co*-RA)-50/50 sample.

Preliminary microscopy observations were performed to study the morphology of the semicrystalline copolymers during their crystallization from the melt. The P(EV-*co*-RA)-50/50 sample was melted and then cooled at 10 °C/min, i.e., at a lower rate with respect to the DSC measurements, in order to better observe the crystallization process. The morphological observations highlighted the ability of the copolymers to form a spherulitic texture, as shown in Figure 6, which displays two images of spherulites growing at two different temperatures, approximately corresponding to the beginning (a) and the end (b) of the crystallization process, during the cooling scan from the melt. Due

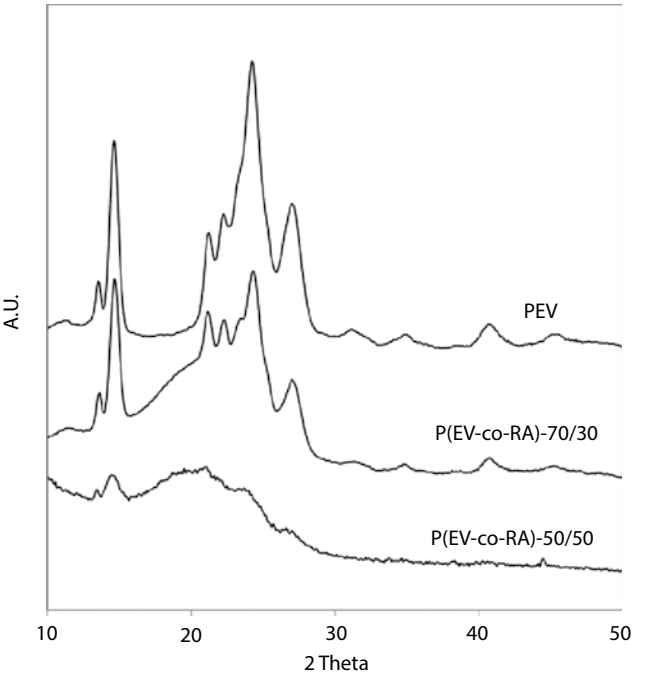

Figure 7 X-ray diffraction patterns of PEV and some P(EV-*co*-RA) copolymers.

to the non-isothermal crystallization, spherulites are characterized by different sizes and complex shapes with irregular edges. It is, however, noteworthy that PEV maintained its ability to crystallize despite the presence of short sequences of EV blocks (Table 2). An average length of EV blocks of about three sequences is sufficient to form a crystalline phase, according to the results obtained for the P(EV-*co*-CL) copolymers. [25]

The X-ray diffraction patterns reported in Figure 7 confirmed the presence of the crystalline structure typical of PEV in the P(EV-*co*-RA)-70/30 sample. The spectrum of the 50/50 sample is characterized by weak reflections, due to its low level of crystallinity (Table 3).

The high capacity of PEV to crystallize in the copolymers confirms the results reported for the

© 2018 Scrivener Publishing LLC

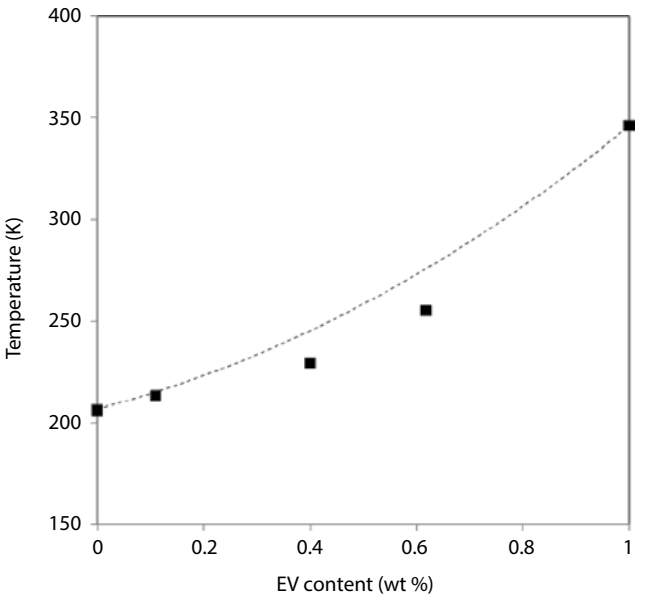

Figure 8 Dependence of T_g of the amorphous samples on composition. The dotted line is calculated using the Fox equation [38].

P(EV-*co*-CL) system, where a weak crystallization process during the second heating scan was also observed for the 20/80 sample [25]. The mobility of EV blocks due to the presence of ether units favors the crystallization process. Moreover, the flexibility of RA units imparts a low viscosity to the system, favoring an ordered arrangement of EV sequences from the melt. A different behavior has been observed in other copolymers, for example, in the PET-*co*-PC system. In this case, the lower mobility of PET chain with respect to that of PEV and the high viscosity of the melt, due to the presence of PC units, prevents the crystallization of PET segments [37].

The crystalline phase, formed during the cooling scan, melts at different T_m in the following heating process, as shown in Figure 5. PEV exhibits a high T_m (264 °C) with a melting peak typical of aromatic polyesters. P(EV-*co*-RA)-70/30 maintains a very high melting temperature, corresponding to a good level of crystal perfection detected by WAXD analysis. A very broad melting process is observed for P(EV-*co*-RA)-50/50, despite the narrow shape of the crystallization peak during the cooling scan. This behavior is not typical of semicrystalline polymers and suggests that different phenomena and processes are present during the second heating scan. For this reason, for this sample the determination of T_m and ΔH_m data was difficult and requires more in-depth study.

Regarding the amorphous phase, after quenching from the melt only one T_g is observed for all the samples. This means that the amorphous phase is homogeneous. Similar results were obtained for the analogous P(EV-*co*-CL) system [25]. The trend of T_g as a function of the copolymers composition, in terms of EV content, is shown in Figure 8, emphasizing that the experimental data fit the Fox equation [38].

4 CONCLUSIONS

This study deals with the synthesis of new copolyesters based on two biobased building blocks, viz. P(EV-*co*RA) random copolymers prepared by a three-component bulk polymerization. The chemical structures of the two monomers is substantially different, the EV units being aromatic and stiff, whereas the RA units bear a flexible long aliphatic chain with a lateral -CH_2- sequence. Despite these differences, the copolymer amorphous phase is homogeneous. Moreover, EV sequences maintain their ability to crystallize even in the presence of a high percentage of RA co-units, whereas RA blocks are always in the amorphous state. Hence, the final properties of these new materials can be easily tuned by modifying the ratio between the two components. Other properties have to be investigated, including their possible antibacterial ability due to the presence of the RA aliphatic side chains. Then, new areas of possible applications for these novel materials could be developed, such as active packaging or biomedical applications.

REFERENCES

1. A. Gandini, The irruption of polymers from renewable resources on the scene of macromolecular science and technology. *Green Chem.* 13, 1061–1083 (2011).
2. A. Gandini and T.M. Lacerda, From monomers to polymers from renewable resources: Recent advances. *Prog. Polym. Sci.* 48, 1–39 (2015).
3. A. Celli, A. Gandini, C. Gioia, T.M. Lacerda, M. Vannini, and M. Colonna, Polymers from pristine and modified natural monomers, in *Chemicals and Fuels from Biobased Buildings Blocks*, F. Cavani, S. Albonetti, F. Basile, and A. Gandini (Eds.), vol. 1, ch. 12, pp. 275–314, Wiley, New Jersey (2016).
4. A. Celli, A. Gandini, C. Gioia, T.M. Lacerda, M. Vannini, and M. Colonna, Polymers from monomers derived from biomass, in *Chemicals and Fuels from Biobased Buildings Blocks*, F. Cavani, S. Albonetti, F. Basile, and A. Gandini (Eds.), vol. 1, ch. 13, pp. 315–344, Wiley, New Jersey (2016).
5. F. Cavani, S. Albonetti, and F. Basile, Aromatics from biomass: Technological options for chemocatalytic transformations, in *Chemicals and Fuels from Biobased Buildings Blocks*, F. Cavani, S. Albonetti, F. Basile, and A. Gandini (Eds.), vol. 1, ch. 2, pp. 33–50, Wiley, New Jersey (2016).
6. M.B. Banella, C. Gioia, M. Vannini, M. Colonna, A. Celli, and A. Gandini, A novel and sustainable route to terephthalic acid precursor. *ChemSusChem* 9, 942–945 (2016).

© 2018 Scrivener Publishing LLC

7. A. Gandini, J.D. Silvestre, C.P. Neto, A.F. Sousa, and M. Gomes, The furan counterpart of poly(ethylene terephthalate): An alternative material based on renewable resources. *J. Polym. Sci. Part A: Polym. Chem.* 47, 295–298 (2009).
8. S. Choi, C.W. Song, J.H. Shin, and S.Y. Lee, Biorefineries for the production of top building block chemicals and their derivatives. *Metab. Eng.* 28, 223–239 (2015).
9. A. Arabi, M. Mizani, and M. Honarvar, The use of sugar beet pulp lignin to the production of vanillin. *Int. J. Biol. Macromol.* 94(A), 345–354 (2017).
10. 10. C. Gioia, M.B. Banella, M. Vannini, A. Celli, M. Colonna, and D. Caretti, Resorcinol: A potentially bio-based building block for the preparation of sustainable polysters. *Eur. Polym. J.* 73, 38–49 (2015).
11. B. Imre, From natural resources to functional polymeric biomaterials. *Eur. Polym. J.* 68, 481–487 (2015).
12. M. Fache, B. Boutevin, and S. Caillol, Vanillin production from lignin and its use as renewable chemical. *ACS Sustain. Chem. Eng.* 4, 35–46 (2016).
13. L. Mialon, A.G. Pemba, and S.A. Miller, Renewable polyethylene terephthalate mimics derived from lignin and acetic acid. *Green Chem.* 12, 1704–1706 (2010).
14. M. Fache, B. Boutevin, and S. Caillol, Vanillin, a key intermediate of biobased polymers. *Eur. Polym. J.* 68, 488–502 (2015).
15. M. Fache, R. Auvergne, B. Boutevin, and S. Caillol, New vanillin diepoxy monomers for the synthesis of of biobased thermosets. *Eur. Polym. J.* 67, 527–538 (2015).
16. B.G. Harvey, A.J. Guenthner, H.A. Meylemans, S.R. Haines, K.R. Lamison, T.J. Groshens, L.R. Cambrea, M.C. Davis, and W.W. Lai, Renewable thermosetting resins and thermoplastics from vanillin. *Green Chem.* 17, 1249–1258 (2015).
17. J.F. Stanzione III, J.M. Sadler, J.J. La Scala, K.H. Reno, and R.P. Wool, Vanillin-based resin for use in composite applications. *Green Chem.* 14, 2346–2352 (2012).
18. C. Zhang, S.A. Madbouly, and M.R. Kessler, Renewable polymers prepared from vanillin and its derivatives. *Macromol. Chem. Phys.* 216, 1816–1822 (2015).
19. C.H.R.M. Wilsens, B.A.J. Noordover, and S. Rastogi, Aromatic thermotropic polyesters based on 2,5-furandicarboxylic acid and vanillic acid. *Polymer* 55, 2432–2439 (2014).
20. N.K. Sini, J. Bijwe, and I.K. Varma, Renewable benzoxazine monomer from vanillin: Synthesis, characterization, and studies on curing behavior. *J. Polym. Sci. Part A: Polym. Chem.* 52, 7–11 (2014).
21. R.S. Jagadish, K.N. Divyashree, P. Viswanath, P. Srinivas, and B. Raj, Preparation of N-vinillyl chitosan and 4-hydroxy benzyl chitosan and their physico-mechanical, optical barrier, and antimicrobial properties. *Carbohydr. Polym.* 87, 110–116 (2012).
22. M. Stroescu, A. Stoica-Guzun, G. Isopencu, S.I. Jinga, O. Parvulescu, T. Dobre, and M. Vasilescu, Chitosan-vanillin composites with antimicrobial properties. *Food Hydrocoll.* 48, 62–71 (2015).
23. A. Prudencio, J.J. Faig, M. Song, and K.E. Uhrich, Phenolic acid based poly(anhydride-esters) as antioxidant materials. *Macromol. Bioisci.* 16, 214–222 (2016).
24. M. Firdaus and M.A.R. Meier, Renewable copolymers derived from vanillin and fatty acid derivatives. *Eur. Polym. J.* 49, 156–166 (2013).
25. C. Gioia, M.B. Banella, P. Marchese, M. Vannini, M. Colonna, and A. Celli, Advances in the synthesis of bio-based aromatic polyesters: Novel copolymers derived from vanillic acid and ε-caprolactone. *Polym. Chem.* 7, 5396–5406 (2016).
26. K.R. Kunduru, A. Basu, M.H. Zada, and A.J. Domb, Castor oil-based biodegradable polyesters. *Biomacromolecules* 16, 2572–2587 (2015).
27. G. Totaro, L. Cruciani, M. Vannini, G. Mazzola, D. Di Gioia, A. Celli, and L. Sisti, Synthesis of castor oil-derived polyesters with antimicrobial activity. *Eur. Polym. J.* 56, 174–184 (2014).
28. L. Sisti, G. Totaro, M. Vannini, L. Giorgini, S. Ligi, and A. Celli, Bio-based PA11/graphene nanocomposites prapared by in situ polymerization. *J. Nanosci. Nanotech.* 18, 1169–1175 (2018).
29. Z.S. Petrovic, I. Cvetkovic, D. Hong, X. Wan, W. Zhang, T. Abraham, and J. Malsam, Polyester polyols and polyurethanes from ricinoleic acid. *J. Appl. Polym. Sci.* 108, 1184–1190 (2008).
30. G. Totaro, L. Paltrinieri, G. Mazzola, M. Vannini, L. Sisti, C. Gualandi, A. Ballestrazzi, S. Valeri, A. Pollicino, A. Celli, D. Di Gioia, and M. L. Focarete, Electrospun fibers containing bio-based ricinoleic acid: Effect of amount and dristribution of ricinoleic acid unit on antibacterial properties. *Macromol. Chem. Eng.* 300, 1085–1095 (2015).
31. M.Y. Krasko and A.J. Domb, Hydrolytic degradation of ricinoleic-sebacic-ester-anhydride copolymers. *Biomacromolecules* 6, 1877–1884 (2005).
32. R. Slivniak and A.J. Domb, Lactic acid and ricinoleic acid based copolyesters. *Macromolecules* 38, 5545–5553 (2005).
33. J. Devaux, P. Godard, and P. Mercier, Bisphenol-A polycarbonate-poly(butylene terephthalate) transesterification. Theoretical study on the structure and on the degree of randomness in four component copolycondensates. *J. Polym. Sci. Part B: Polym. Phys.* 20, 1875–1880 (1982).
34. H. Tsuji, T. Yamada, M. Suzuki, and S. Itsuno, Effects of poly(L-lactide-co-ε-caprolactone) on morphology, structure, crystallization, and physical properties of blends of poly(L-lactide) and poly(ε-caprolactone). *Polym. Int.* 52, 269–275 (2003).
35. H. Tsuji, A. Mizuno, and Y. Ikada, Enhanced crystallization of poly(L-lactide-ε-caprolactone) during storage at room temperature. *J. Appl. Polym. Sci.* 76, 947–953 (2000).
36. H.R. Kricheldorf and I. Kreiser, Transesterification of poly (L-lactide) with poly(glycolide), poly(β-propiolactone), and poly(ε-caprolactone). *J. Macromol. Sci. Part A: Pure Appl. Chem.* **24**, 1357–1367 (1987).
37. A. Celli and P. Marchese, Crystallization of poly(ethylene terephthalate) in poly(ethylene terephthalate)/bisphenol A polycarbonate block copolymers: Influence of block length and role of the rubbery amorphous component. *Macromol. Chem. Phys.* 205, 2486–2495 (2004).
38. T.G. Fox, Influence of diluent and of copolymer composition on the glass temperature of a polymer system. *Bull. Am. Phys. Soc.* 1, 123–132 (1956).

 © 2018 Scrivener Publishing LLC